JOURNAL OF APPLIED ELECTROCHEMISTRY 25 (1995) 326–333

Calculation of the impedance of noncylindrical pores Part I: Introduction of a matrix calculation method

K. ELOOT, F. DEBUYCK, M. MOORS, A. P. VAN PETEGHEM

Laboratorium voor Non-Ferro Metallurgie, Universiteit Gent, Campus Ardoyen, Technologiepark-Zwijnaarde 9, B-9052 Zwijnaarde, Belgium

Received 13 April 1994; revised 21 September 1994

In this paper a new method is proposed for the calculation of the impedance of arbitrary electrodes containing noncylindrical pores and/or having place-dependent impedances. The method is based on splitting up the pore and the surrounding material into N discs. For the equivalent circuit of each disc a transmission line with constant impedances is adopted. By matrix calculations the impedance of the porous electrode can be obtained. A comparison is made between this, very general, matrix method and a recursion method developed by Keiser *et al.* for purely capacitive interface behaviour of pores in an electrode material with negligible impedance. It is shown that the matrix method requires much smaller N-values owing to the use of transmission lines for each disc. This makes it more appropriate to be used in curve fitting procedures. Moreover, it is shown that the typical behaviour of the pore impedance at low penetration depths is much better simulated with the matrix method. Furthermore, an attempt is made to provide more general knowledge about the impedance behaviour of noncylindrical pores as a function of the penetration depth of the a.c. signal. Finally, the theory is enlarged using constant phase elements instead of capacities to describe the behaviour of the electrode/electrolyte interfaces.

1. Introduction

Over the last thirty years different researchers have reported the calculation of the impedance of porous electrodes. De Levie [1–3] studied pores with a constant section in a material with negligible resistance. He justified the one-dimensional modelling of the electrochemical system. As a consequence, the impedance of the porous electrode could be described as a parallel combination of the impedances of the different pores. For the impedance of a single pore, a transmission line was adopted. It was shown that with decreasing frequency the current penetrates deeper into the pore, making it possible to obtain information on the pore shape from impedance measurements.

Keiser *et al.* [4] calculated the impedance of noncylindrical pores as a function of the penetration depth λ of the a.c. signal (Fig. 1). They supposed the pores to be solids of revolution and calculated their impedance using a recursion formula. The electrode material was again assumed to have a negligible resistance. The disadvantage of this calculation method is the fact that the electrochemical system was not only geometrically, but also electrochemically, simplified. Geometric simplification consists of splitting the pore into N discs with height l/N (l is the pore length) and disc-dependent radius r_i ($1 \leq i \leq N$). Electrochemical simplification consists in the use of a combination of noninfinitesimal impedances as equivalent circuit for each disc, instead of using a transmission line with infinitesimal impedances for each disc.

In this paper a new method is described for the calculation of the impedance of noncylindrical pores in electrodes with nonnegligible electrode impedance. The calculation method is based only on a geometrical simplification and is called the matrix method. In addition to recent literature [5–9] a variable pore section and the possibility of impedance changes over the pore depth are taken into account in this matrix method.

In other papers the described method will be used to evaluate the impedance behaviour of both cylindrical and non-cylindrical scaled-up pores drilled in stainless steel (Part II, [10]) and of porous and sealed anodization layers on aluminium [11].

2. Model description

2.1. *Matrix method for the calculation of the pore impedance*

For the calculation of the impedance of porous electrodes in an electrolyte solution it is assumed that the pores are homogeneously filled with electrolyte. Moreover, the equipotential planes inside the electrolyte and material phase are assumed to lie perpendicular to the pore axis. These assumptions are an extension of those made for electrodes with negligible resistance [3]. They allow one-dimensional modelling of the electrochemical system.

0021-891X

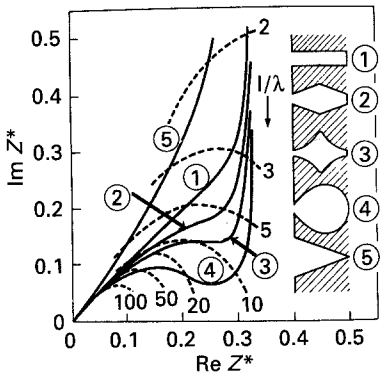

Fig. 1. Nyquist curves for the normalized pore impedance by Keiser *et al.* [4] (l is the pore length, λ is the penetration depth of the a.c. signal).

The porous electrode, soaked with electrolyte, can be assumed to be a parallel combination of pores surrounded by an appropriate amount of electrode material. The translation of this system into an equivalent electrical circuit has to take into account that the impedance of the porous electrode can be seen as a parallel combination of the impedances of different pores. These can have different dimensions and theoretically even different shapes.

It is assumed that an electrode with thickness d (cm) and surface area A (cm^2) contains a pore having the shape of a solid of revolution. The pore has a depth l (cm) and a radius $r(x)$, which can change over the depth. The similarity between the electrochemical system and the equivalent circuit is shown in Fig. 2. This was obtained by translating all the electrical and electrochemical phenomena into suitable impedances.

In the equivalent circuit (Fig. 3) I stands for the total current through a section (A), R_e is the electrolyte resistance (Ω), x the position coordinate (cm), l the pore depth (cm), $R_s(x)$ the electrolyte resistance in the pore per unit length ($\Omega\,\mathrm{cm}^{-1}$), $Z_m(x)$ the material impedance round the pore per unit length ($\Omega\,\mathrm{cm}^{-1}$), $Z(x)$ the interface impedance for a unit length of pore (Ω cm), Z_I the impedance of the electrode surface round the pore mouth (Ω), Z_U the impedance of the pore base (Ω), Z_b the material layer impedance (Ω), $i_m(x)$ and $i_s(x)$ the currents flowing, respectively, into the electrode material and the electrolyte. The position dependence of the impedances R_s, Z_m and Z can be due to the position dependence of the pore section and to that of the specific impedances.

The calculation of the pore impedance Z_p was carried out using a finite element approach. The elements were obtained by splitting the pore and the surrounding electrode material into N discs. These may have different heights, which was not the case for the model of Keiser *et al.* [4]. Material element i ($1 \le i \le N$) lies between $x = a_i$ and $x = b_i$, has a thickness $l_i = b_i - a_i$ and contains an electrolyte disc with radius r_i. The surrounding material has a surface area $A_i = A - \pi r_i^2$. The equivalent circuit of each of these elements is a transmission line, $\mathrm{TL}^{(i)}$,

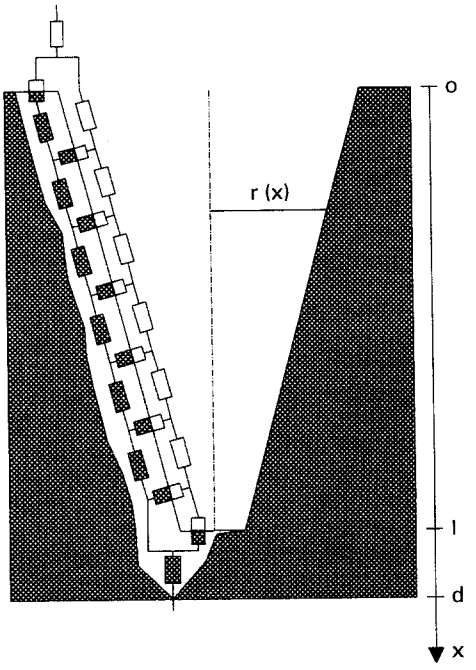

Fig. 2. A transmission line as equivalent circuit for the impedance of an electrode with nonnegligible material impedance containing a pore with variable radius.

with constant parameters $Z_m^{(i)}$, $Z^{(i)}$ and $R_s^{(i)}$ (Fig. 4(a), ϕ is the potential difference across the interface (V)). Such a TL with constant parameters has already been described in the literature [5–9].

The inlet of the five gate $\mathrm{TL}^{(i)}$ is characterized by the parameters $I_s^{(i-1)}$, $\phi^{(i-1)}$ and $I_m^{(i-1)}$, from which all the currents and voltages inside $\mathrm{TL}^{(i)}$ can be calculated (Fig. 4(b)). As a consequence, the outlet parameters $I_s^{(i)}$ and $\phi^{(i)}$ can also be written as functions of $I_s^{(i-1)}$, $\phi^{(i-1)}$ and $I_m^{(i-1)}$,

$$\begin{bmatrix} I_s^{(i)} \\ \phi^{(i)} \\ I \end{bmatrix} = \begin{bmatrix} C^{(i)} & -S^{(i)}\dfrac{\chi_k^{(i)}}{Z^{(i)}} & D^{(i)}(1-C^{(i)}) \\ -S^{(i)}\dfrac{Z^{(i)}}{\chi_k^{(i)}} & C^{(i)} & S^{(i)}\chi_k^{(i)}Z_m^{(i)} \\ 0 & 0 & 1 \end{bmatrix} \times \begin{bmatrix} I_s^{(i-1)} \\ \phi^{(i-1)} \\ I \end{bmatrix} \tag{1}$$

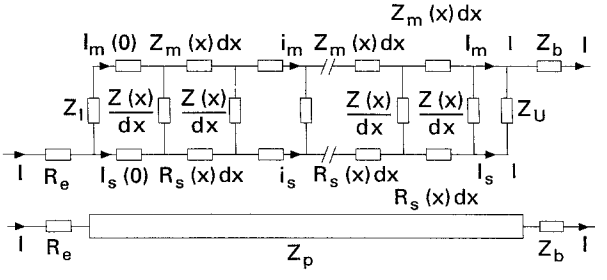

Fig. 3. Equivalent circuit for the measured impedance.

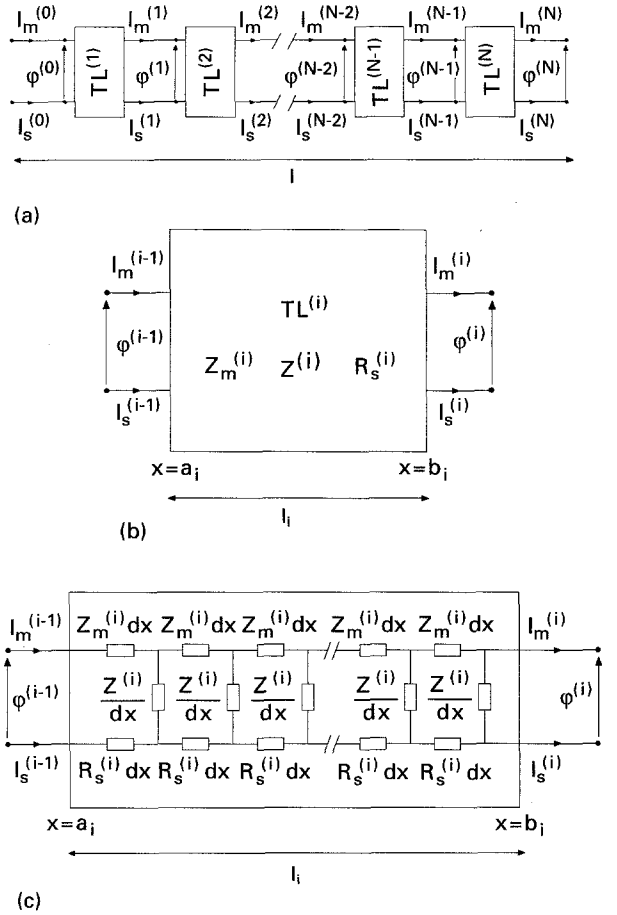

Fig. 4. (a) Splitting the pore into N parts means dividing the transmission line with variable parameters into N transmission lines with constant parameters. (b, c) Equivalent circuit adopted for disc i.

with

$$\chi_k^{(i)} = \sqrt{\left(\frac{Z^{(i)}}{Z_m^{(i)} + R_s^{(i)}}\right)} \quad \text{and} \quad D^{(i)} = \frac{Z_m^{(i)}}{Z_m^{(i)} + R_s^{(i)}} \tag{2,3}$$

$$S^{(i)} = \sinh\left(\frac{l_i}{\chi_k^{(i)}}\right) \quad \text{and} \quad C^{(i)} = \cosh\left(\frac{l_i}{\chi_k^{(i)}}\right) \tag{4,5}$$

Since the pore is divided into N discs,

$$\begin{bmatrix} I_s^{(N)} \\ \phi^{(N)} \\ I \end{bmatrix} = \prod_{i=N}^{1} \begin{bmatrix} C^{(i)} & -S^{(i)}\dfrac{\chi_k^{(i)}}{Z^{(i)}} & D^{(i)}(1 - C^{(i)}) \\ -S^{(i)}\dfrac{Z^{(i)}}{\chi_k^{(i)}} & C^{(i)} & S^{(i)}\chi_k^{(i)} Z_m^{(i)} \\ 0 & 0 & 1 \end{bmatrix} \times \begin{bmatrix} I_s^{(0)} \\ \phi^{(0)} \\ I \end{bmatrix} \tag{6}$$

It is worth noting that the product has to be taken from N to 1, i.e., from the end to the beginning of the pore. In symbolic notation Equation 6 is written as,

$$I_s^{(N)} = \alpha I_s^{(0)} + \beta\phi^{(0)} + \gamma I \tag{7}$$

$$\phi^{(N)} = \epsilon I_s^{(0)} + \eta\phi^{(0)} + \nu I \tag{8}$$

Equations 7 and 8 contain four unknown parameters. Two other equations can be found from Ohm's law at the pore mouth and pore base (Fig. 3),

$$\phi^{(0)} = Z_I(I - I_s^{(0)}) \tag{9}$$

$$\phi^{(N)} = Z_U I_s^{(N)} \tag{10}$$

Since all voltages and all currents are proportional to I, we can write,

$$\phi^{(i)} = \underline{\phi^{(i)}} \cdot I \tag{11}$$

$$I_s^{(i)} = \underline{I_s^{(i)}} \cdot I \tag{12}$$

The total impedance Z_p of the pore embedded in the surrounding material is then given by

$$Z_p = \underline{\phi^{(N)}} - \sum_{i=1}^{N} R_s^{(i)} \chi_k^{(i)} \frac{C^{(i)} - 1}{S^{(i)}} [2D^{(i)} - \underline{I_s^{(i)}} - \underline{I_s^{(i-1)}}] + \sum_{i=1}^{N} R_s^{(i)} D^{(i)} l_i \tag{13}$$

From this expression, the impedance of a porous electrode can be calculated taking into account the parallel combination of the different pores. For the case of cylindrically shaped pores this is worked out in [5–8].

2.2. *Comparison with the recursion formula of Keiser et al. [4]*

Keiser *et al.* [4] proposed a recursion formula for the calculation of the impedance of a noncylindrical pore in an electrode with negligible impedance ($Z_m = 0$). The pore was supposed to have the shape of a solid of revolution and the interface impedance Z was taken purely capacitive. Moreover, both the electrode material around the pore mouth and the pore base were assumed to behave as insulators ($|Z_I| = \infty$, $|Z_U| = \infty$). Using the assumptions made above, a comparison between the recursion method and the matrix method can be made.

2.2.1. Recursion method. For the calculation of the pore impedance Keiser *et al.* divided the pore into N discs with height l/N and radius r_i ($1 \leq i \leq N$). Each disc has its own electrolyte resistance and interface capacity. The standardized pore impedance Z_* ($=Z_*^{(0)}$) can be found by using the recursion formula,

$$Z_*^{(i-1)} = \frac{1}{Ng_i^2} + \frac{1}{j\dfrac{1}{2N}\left(\dfrac{1}{\lambda_r}\right)^2 g_i + \dfrac{1}{Z_*^{(i)}}} \tag{14}$$

Since the pore base behaves as an insulator ($|Z_U| \to \infty$), the starting impedance of the recursion formula is given by

$$\frac{1}{Z_*^{(N)}} = 0 \tag{15}$$

The standardization mentioned above consists in

dividing the pore impedance by the resistance of the electrolyte cylinder having the same mean radius r and depth l as the noncylindrical pore,

$$Z_*^{(i)} = \frac{Z_p^{(i)}}{R_0} \tag{16}$$

$$R_0 = \frac{\rho_s l}{\pi r^2} \tag{17}$$

ρ_s is the specific electrolyte resistance (Ω cm).

In Equation 14 a dimensionless shape factor g_i and the penetration depth λ_r of the a.c. signal are used, given by,

$$g_i = \frac{r_i}{r} \tag{18}$$

$$\lambda_r = \frac{1}{2}\sqrt{\frac{r}{\rho_s \omega C_w}} \tag{19}$$

ω is the circular frequency (rad s^{-1}) and C_w is the double layer capacity per unit surface (F cm^{-2}).

2.2.2. Matrix method. In the matrix method the pore is also divided into N discs with radius r_i ($1 \leq i \leq N$) which can now have different heights l_i. The assumption that the electrode material has a negligible impedance ($Z_m^{(i)} = 0, \quad i = 1, \ldots, N$) simplifies Equation 6 to

$$\begin{bmatrix} I_s^{(N)} \\ \phi^{(N)} \end{bmatrix} = P^{(N)} \prod_{i=N}^{1} \begin{bmatrix} 1 & -T^{(i)} \dfrac{\lambda_k^{(i)}}{Z^{(i)}} \\ -T^{(i)} \dfrac{Z^{(i)}}{\lambda_k^{(i)}} & 1 \end{bmatrix} \times \begin{bmatrix} I_s^{(0)} \\ \phi^{(0)} \end{bmatrix} \tag{20}$$

with

$$\lambda_k^{(i)} = \sqrt{\frac{Z^{(i)}}{R_s^{(i)}}} \tag{21}$$

$$Z^{(i)} = \frac{Z_w}{2\pi r_i} \tag{22}$$

$$R_s^{(i)} = \frac{\rho_s}{\pi r_i^2} \tag{23}$$

and

$$T^{(i)} = \tanh\left(\frac{l_i}{\lambda_k^{(i)}}\right) \tag{24}$$

$$P^{(N)} = \prod_{i=1}^{N} \cosh\left(\frac{l_i}{\lambda_k^{(i)}}\right) \tag{25}$$

$\lambda_k^{(i)}$ is the complex penetration depth of the a.c. signal in the ith disc. Z_w is the specific interface impedance (Ω cm^2). After multiplication Equation 20 can be written as,

$$\begin{bmatrix} I_s^{(N)} \\ \phi^{(N)} \end{bmatrix} = P^{(N)} \begin{bmatrix} \alpha' & \beta' \\ \epsilon' & \eta' \end{bmatrix} \begin{bmatrix} I_s^{(0)} \\ \phi^{(0)} \end{bmatrix} \tag{26}$$

In the case of an electrode with negligible impedance the impedance, Z_I, of the electrode surface around the pore mouth is connected parallel with the pore impedance. It is thus possible to take this impedance into account afterwards and suppose Z_I to be infinite in the subsequent calculation. The boundary conditions are then,

$$I_s^{(0)} = I \tag{27}$$

$$\phi^{(N)} = Z_U I_s^{(N)} \tag{28}$$

Combining Equations 26, 27 and 28 and $Z_p = \phi^{(0)}/I$ the pore impedance can be written as

$$Z_p = -\frac{\epsilon' - Z_U \alpha'}{\eta' - Z_U \beta'} \tag{29}$$

For the special case of an insulating pore base ($|Z_U| = \infty$) the pore impedance Z_p and the standardized pore impedance Z_* become

$$Z_p = -\frac{\alpha'}{\beta'} \tag{30}$$

$$Z_* = \frac{-1}{R_0}\frac{\alpha'}{\beta'} \tag{31}$$

For a cylindrical pore Equations 29 and 30 are, respectively, reduced to

$$Z_p = Z_\infty \frac{Z_U C + Z_\infty S}{Z_U S + Z_\infty C} \tag{32}$$

for a pore base with impedance Z_U and to

$$Z_p = Z_\infty \frac{C}{S} \tag{33}$$

for an insulating pore base.

In Equations 32 and 33 Z_∞ is the impedance of an infinitely deep cylindrical pore [1–3],

$$Z_\infty = \sqrt{(Z R_s)} \tag{34}$$

3. Discussion

For the recursion method a purely capacitive interface was assumed. However, up to now no assumption was made concerning the interface of the pore in the matrix method. Assuming a capacitive interface and an insulating pore base, the standardized pore impedance Z_* can be calculated for various pore geometries, both with the recursion method and the matrix method.

Z_*, given by Equation 14, depends only on l/λ_r, the pore geometry g_i and the number of discs N. This means that for uniform pores the same standardized pore impedance is found, as a function of l/λ_r. It can be shown that sufficient conditions for this property are that the specific interface impedance Z_w (Ω cm^2) is not a purely resistive constant-phase element (CPE, $Z_w = Q_w = Q_{0,w}\,(j\omega)^{-\alpha}$, $-1 \leq \alpha \leq 1$ and $\alpha \neq 0$) and that the pore base is an insulator. In this case the real penetration depth λ_r is given by

$$\lambda_r = \sqrt{\left(\frac{Q_{0,w} r}{2\rho_s \omega^\alpha}\right)} \cos\left(\alpha \frac{\pi}{4}\right) \tag{35}$$

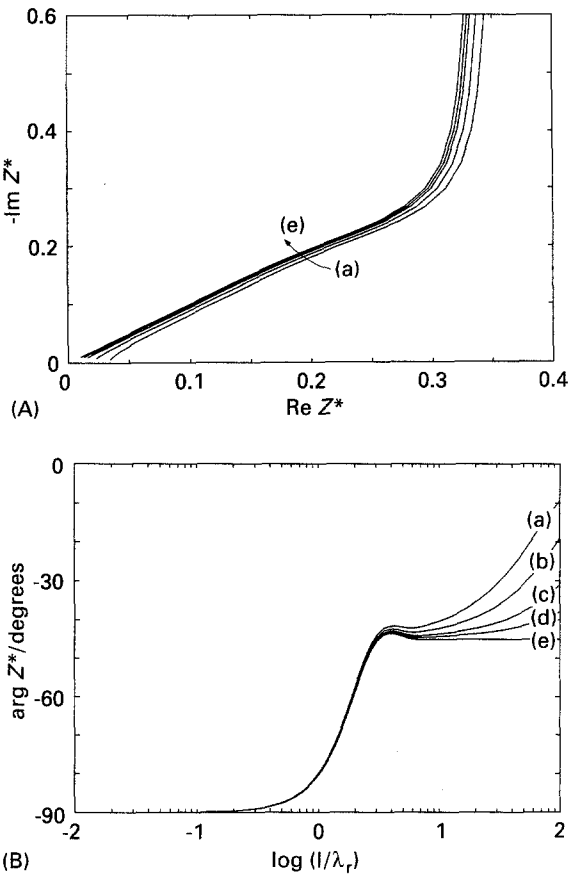

Fig. 5. Comparison between the analytically calculated normalized pore impedance and the one calculated for different N values with the recursion method ($\alpha = 1$) for the case of a cylindrical pore. (A) Nyquist plot. (B) Bode phase plot. N: (a) 30, (b) 50, (c) 100, (d) 200 and (e) analytical solution.

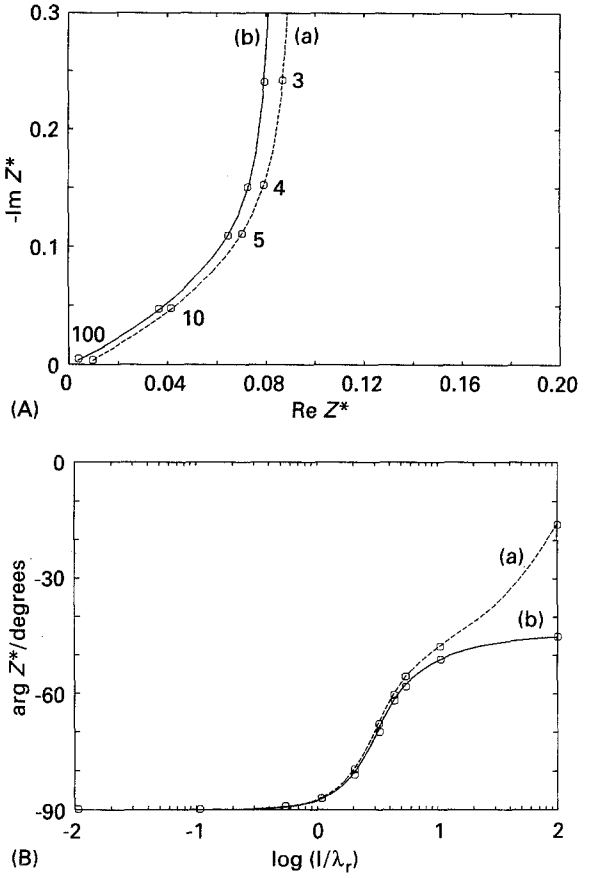

Fig. 6. Comparison between the normalized pore impedance ($\alpha = 1$) for a conically shaped pore calculated with the recursion method ($N = 30$) and with the matrix method ($N = 20$). (A) Nyquist plot. (B) Bode phase plot. Key: (a) recursion, (b) matrix and (○) l/λ_r in (A).

Experimental samples of pores with CPE interface behaviour will be given in part II. A purely capacitive interface, as is the assumption of Keiser *et al.*, results in a special CPE with $\alpha = 1$ and $Q_{0,w} = 1/C_w$. Equation 35 then simplifies to Equation 19.

Using Equation 35, the pore impedance, calculated with the matrix method as a function of the frequency f or the circular frequency ω, can also be written as function of $1/\lambda_r$.

Keiser *et al.* claim that for simple pore geometries splitting the pore into 30 to 40 cells is sufficient. Since the impedance of a cylindrical pore can be calculated analytically, a justification of this assertion can be made by calculating the impedance for different N-values (Fig. 5). It is seen that the curve found with the recursion formula for $N = 30$ is not going to the origin of the coordinate system. It produces a serial resistance given by $1/Ng_1^2$. This resistance becomes zero if N is infinite. However, at high enough values of l/λ_r, thus very small penetration depths, the pore behaves as an infinitely deep cylindrical one [2, 3]. The standardized and nonstandardized impedance are then,

$$Z_{*,\infty} = \left[1 + j\tan\left(-\alpha\frac{\pi}{4}\right)\right]\frac{\lambda_r}{l} \quad (36)$$

$$Z_{p,\infty} = Z_{*,\infty}R_0 \quad (37)$$

Since it is seen in Equation 35 that λ_r is proportional to $\omega^{-\alpha/2}$ it is concluded that these impedances represent a CPE with half the exponent of Q_w. As can be seen from Figs 5 to 8 this is the case for the pore impedance calculated using the matrix method ($\alpha = 1$, resulting in a $-45°$ phase angle). However, when the recursion formula is used, the influence of the serial resistance is so big that the typical infinitely deep pore behaviour is hardly visible in the phase diagram for N-values proposed by Keiser *et al.*

For arbitrary pore geometries no analytical solution exists. For a conical pore ($r(l) = 0$) the comparison between the impedance calculated with the recursion formula and that calculated with the matrix method is shown in Fig. 6. In Fig. 7 this is done for a pore with geometry b (see Fig. 9). It is shown in Fig. 8 that for a pore with a pore mouth much smaller than the pore base (case c of Fig. 9) the serial resistance becomes relatively large. Extraction of this serial resistance from the calculated pore impedance does not result in a correction. This would affect the limiting value of $\mathrm{Re}(Z_*)$ for $l/\lambda_r \to 0$ which was found to depend on the pore geometry. In this we disagree with Keiser *et al.*, who reported that: "Using an appropriate standardization of the pore shape factor $g(\xi)$ as given by Equation 18, always the same limiting value is reached for the real part of Z_*." They illustrated this using Fig. 1. However, this figure is not correct.

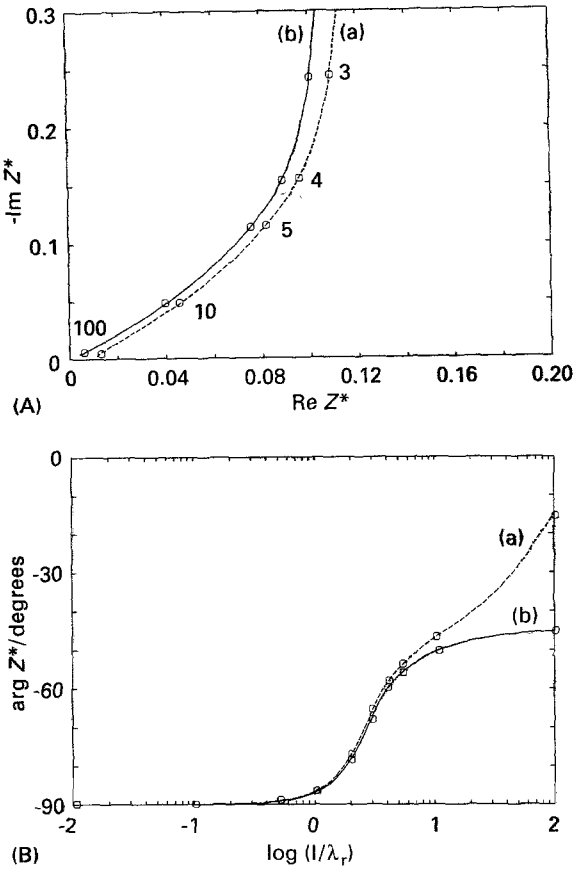

Fig. 7. Comparison between the normalized pore impedance ($\alpha = 1$) for a pore with shape b (Fig. 9) calculated with the recursion method ($N = 30$) and with the matrix method ($N = 20$). (A) Nyquist plot. (B) Bode phase plot. Key: as for Fig. 6.

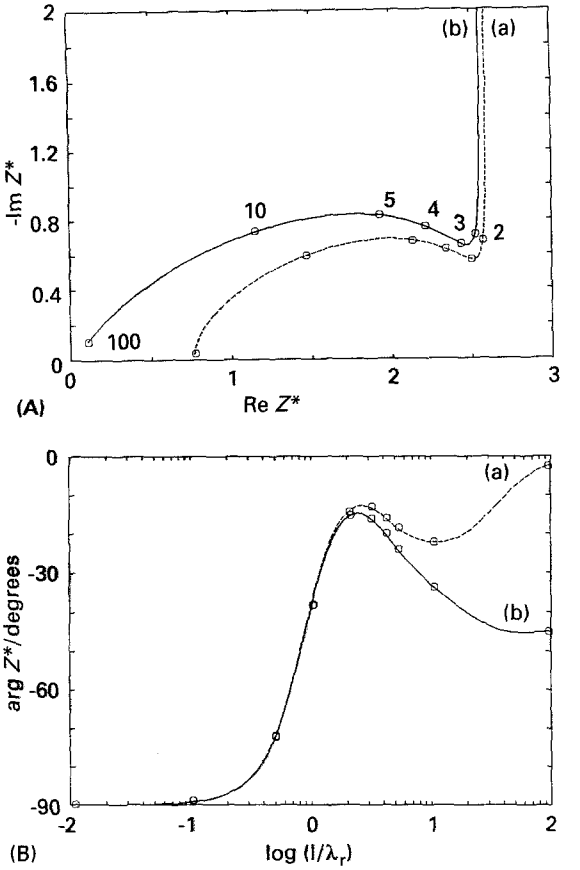

Fig. 8. Comparison between the normalized pore impedance ($\alpha = 1$) for a pore with shape c (Fig. 9) calculated with the recursion method ($N = 30$) and with the matrix method ($N = 20$). (A) Nyquist plot. (B) Bode phase plot. Key: as for Fig. 6.

It is clear that the real part of Z_* can only be due to the resistance behaviour of the electrolyte inside the pore, since the pore wall was supposed to be purely capacitive. As a consequence, a small standardized pore radius $g(\xi = 0)$ at the pore mouth increases the real part of Z_* much more than the same pore radius $g(\xi = 1)$ at the pore base. This is due to the flattening of the a.c. signal from the top to the bottom of the pore (Fig. 10). As a consequence, geometry b (Fig. 9) results in a smaller real part of Z_* than geometry c ($g_{N-i+1}(\mathrm{c}) = g_i(\mathrm{b})$).

The limiting value of $\mathrm{Re}(Z_*)$ for $l/\lambda_r \to 0$ and $\alpha = 1$ is found to equal a number that only depends on the pore form. This number is called the geometry constant Λ_g and given by the weighted average of ratios V_i

$$\Lambda_g = \lim_{1/\lambda_r \to 0} \mathrm{Re}\,[Z_*] = \lim_{N \to \infty} \left[\frac{1}{N} \sum_{i=1}^{N} \left(\frac{N-i+1}{N} \right)^2 V_i \right] \tag{38}$$

with

$$V_i = \frac{\pi \left(\dfrac{\sum_{j=i}^{N} g_j}{N-i+1} \right)^2}{\pi g_i^2} \tag{39}$$

V_i is the ratio of the surface of the circle which has a radius equal to the mean radius of the cylinders i to N to the surface of the ith cylinder. According to Equation 38 the surface ratio V_1, at the inlet of the pore, has the biggest weight of all ratios, thus resulting in a geometry-dependent real part of the standardized pore impedance.

$\Lambda_g = 1/3$ for a cylindrical pore, since all ratios V_i are given by $V_i = 1$ $(1 \le i \le N)$. A pore with narrowing cross section has $V_i < 1$ $(1 \le i \le N-1)$ and $V_N = 1$, resulting in $\Lambda_g < 1/3$, as can be seen in Fig. 7(A). A pore with broadening cross section has $V_i > 1$ $(1 \le i \le N-1)$ and $V_N = 1$, resulting in $\Lambda_g > 1/3$, as can be seen in Fig. 8(A). This will be proved experimentally in Part II.

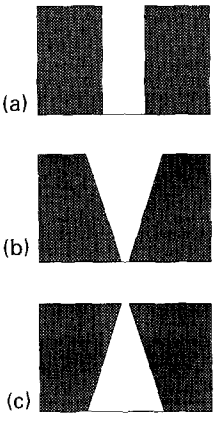

Fig. 9. Pores with different $r(0)/r(l)$ ratios. The pores are drawn so that they have the same mean radius. (a) $r(0)/r(l) = 1$; (b) $r(0)/r(l) = 10$; (c) $r(0)/r(l) = 0.1$.

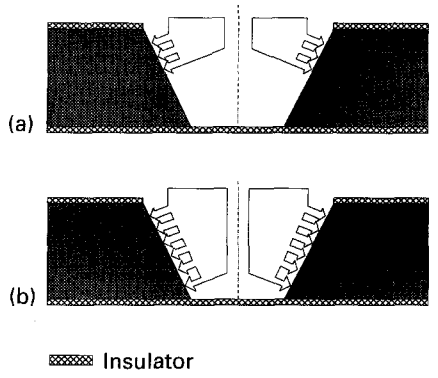

Fig. 10. View of the current flow in the pore filled with electrolyte as a function of decreasing frequency (i.e. increasing penetration depth).

For the calculation of Λ_g it is more appropriate to use the matrix method than to use Equation 38, which is the result of the recursion formula of Keiser *et al.* Using the matrix method, Λ_g is given by the real part of the standardized pore impedance Z_* when a purely capacitive interface is assumed and $l/\lambda_r = 10^{-2}$. For a conical pore (Fig. 6(A), $\Lambda_g = 1/12 \approx 0.0833$) the matrix method provides $\Lambda_g \approx 0.0834$ for $N = 100$, whereas with Equation 38 $\Lambda_g \approx 0.0835$ is found for $N = 2000$. The calculation time is thus reduced 20 times when the matrix method is used.

In contrast with the real part of Z_* the limit of the imaginary part is independent of the pore shape, as can be seen in the case of a capacitive interface

$$\omega \ll, \frac{l}{\lambda_r} \ll: \; Z_* = \Lambda_g - j\left(\frac{\lambda_r}{l}\right)^2 \tag{40}$$

$$Z_p = \Lambda_g R_0 + \frac{1}{2\pi r l}\frac{1}{j\omega C_w} \tag{41}$$

It is seen that for large penetration depths the pore wall behaves as a flat surface with area $2\pi rl$ and specific interface impedance $1/(j\omega C_w)$. Its impedance is connected in series with $\Lambda_g R_0$. It is obvious that $1/(j\omega C_w)$ can be replaced in Equation 41 by an arbitrary specific interface impedance Z_w,

$$\omega \ll, \frac{l}{\lambda_r} \ll: \; Z_p = \Lambda_g R_0 + \frac{Z_w}{2\pi r l} \tag{42}$$

An example of this will be given experimentally and theoretically in Part II for a Z_w given by the parallel combination of a CPE and a resistance.

To summarize, the pore impedance was calculated for different pore forms (Fig. 11), assuming a purely capacitive interface behaviour. It is seen that for very small penetration depths the pore impedance behaves as the impedance of an infinitely deep pore ($Z_p \approx Z_\infty$) resulting in the phase angle $-45°$, independent of the pore shape. With decreasing frequency the penetration depth of the a.c. signal increases. In this way the pore shape is 'scanned' as a function of penetration depth. It is seen clearly in Fig. 11(C) that a narrowing (broadening) pore section results in a decrease (increase) of the phase angle, which is negative. As a consequence, the phase angle

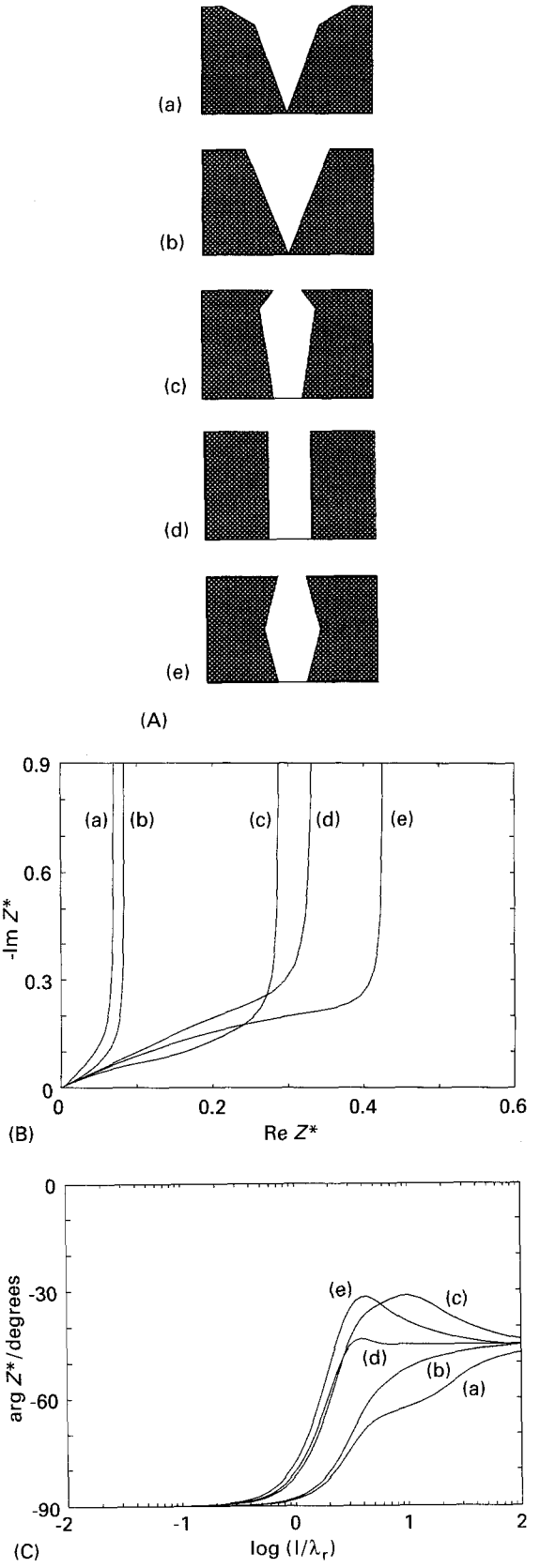

Fig. 11. Comparison of the normalized pore impedances of different pore shapes calculated with the matrix method. (A) The pore shapes. (B) Nyquist plot. (C) Bode phase plot.

becomes smaller (larger) than $-45°$ for a pore which narrows (broadens) at the pore mouth. In the more general case of a CPE $-45°$ has to be replaced by $-\alpha 45°$, according to Equation 36. This will be illustrated in Part II. Finally, it is seen that the real part

of Z_* becomes a constant for large penetration depths. This constant is Λ_g. The imaginary part of Z_* shows 'flat surface behaviour', independent of the pore form, since a vertical line in a Nyquist plot is connected with purely capacitive behaviour.

4. Summary and conclusions

A new method is developed for the calculation of the impedance of arbitrary electrodes containing noncylindrical pores and/or having position-dependent impedances. Compared to the recursion method of Keiser *et al.* [4] for a perfectly conducting electrode material the matrix method is more general and has the advantage that a transmission line is adopted as equivalent circuit for each disc obtained by splitting up the pore. This results in a substantial reduction of the minimally required number of discs. As a consequence curve fitting and impedance simulation time are decreased at least 10 times. Meanwhile, a better simulation of the typical behaviour of the pore impedance at low penetration depths is obtained.

More general knowledge is provided about the impedance behaviour of noncylindrical pores in perfectly conducting material as a function of the penetration depth of the a.c. signal. It is noted that uniform pores have the same standardized pore impedance provided the pore base is an insulator and the interface impedance is a nonpurely resistive CPE. Moreover, it is found that a statement of Keiser *et al.* has to be corrected. The boundary value of the real part of the standardized pore impedance in the case of a capacitive interface is not independent of the pore geometry. As a consequence, a geometric constant is introduced and its meaning is explained.

References

[1] R. de Levie, *Electrochim. Acta* **8** (1963) 751.
[2] *Idem, ibid.* **9** (1964) 1231.
[3] *Idem, Adv. Electrochem. & Electrochem. Engng* **6** (1967) 329.
[4] H. Keiser, K. D. Beccu and M. A. Gutjahr, *Electrochim. Acta* **21** (1976) 539.
[5] J. R. Park and D. D. Macdonald, *Corros. Sci.* **23** (1983) 295.
[6] S. J. Lenhart, D. D. Macdonald and B. G. Pound, *J. Electrochem. Soc.* **135** (1988) 1063.
[7] C. Cachet, B. Saidani and R. Wiart, *J. Electrochem. Soc.* **139** (1992) 644.
[8] J. G. Thevenin and R. H. Muller, *ibid.* **134** (1987) 2650.
[9] F. Mansfeld and M. W. Kendig, *ibid.* **135** (1988) 828.
[10] K. Eloot, F. Debuyck, M. Moors and A. P. Van Peteghem, Part II, *J. Appl. Electrochem.* **25** (1995).
[11] F. Debuyck, K. Eloot, M. Moors and A. P. Van Peteghem, to be published.